ROYAL SOCIETY
OF CHEMISTRY

Soft Matter

A Broader View on Jamming: From Spring Networks to Circle Packings

SCHOLARONE™
Manuscripts

Soft Matter

ROYAL SOCIETY OF CHEMISTRY

ARTICLE TYPE

A Broader View on Jamming: From Spring Networks to Circle Packings†

Varda F. Hagh,[*a] Eric I. Corwin,[b‡] Kenneth Stephenson,[c‡] and M. F. Thorpe[a,d]

Jamming occurs when objects like grains are packed tightly together (e.g. grain silos). It is highly cooperative and can lead to phenomena like earthquakes, traffic jams, etc. In this paper we point out the paramount importance of the underlying contact network for jammed systems; the network must have one contact in excess of isostaticity *and* a finite bulk modulus. Isostatic means that the number of degrees of freedom is exactly balanced by the number of constraints. This defines a large class of networks that can be constructed without the necessity of packing particles together compressively (either in the lab or computationally). One such construction, which we explore here, involves setting up the Delaunay triangulation of a Poisson disk sampling and then removing edges to maximize the bulk modulus until the isostatic plus one edge is reached. This construction works in any dimensions and here we give results in $2D$ where we also show how such networks can be transformed into disk packs.

1 Introduction

Amorphous materials are ubiquitous in nature, spanning such disparate systems as granular media[1], foams[2], colloidal suspensions[3], and glasses[4]. Two decades ago it was suggested that the jamming transition unified all of these systems into a common framework[5]. Through this lens, one can see that many amorphous materials share unusual mechanical and vibrational properties at the transition from flowing to rigid, marked by the vanishing ratio of the shear to bulk modulus[6] and the development of an excess of low frequency vibrational modes about the Boson peak[7–9]. For most amorphous systems, the external control parameter which controls this transition is the packing fraction or density of particles. However, recent results demonstrate that density alone does not directly control the properties of the transition[1]. Instead, changes in density induce a change in the underlying connectivity network and it is this underlying network that determines the rigidity and related responses of any given system.

Disordered packings of athermal frictionless particles are a standard model for studying the jamming transition in amorphous materials. Every jammed system has a corresponding elastic network that renders the physical properties of the original

system[10,11]. Such networks are created by replacing the center of mass of each particle with a vertex and adding a spring edge between two vertices if their equivalent particles are in contact. The spring network is a simple yet powerful model to study the mechanical and vibrational properties of materials with dominant short range interactions which is the case for the jammed systems. The spring network model provides a linearized picture of the complex physical systems and allows a full description of the mechanical response and rigidity of the material structures in terms of their geometry[12,13]. The mechanical response of a spring network to any external deformation can be calculated by solving the set of linear equations of motions for the vertices while taking into account the forces applied on each vertex by the springs that are connected to it[14]. The rigidity of a spring network, on the other hand, can be studied by looking at the balance between its degrees of freedom and constraints. In a d dimensional network with N vertices, each vertex has d degrees of freedom. Therefore, the total number of degrees of freedom is dN. Connecting any pair of vertices with a spring imposes a constraint on their rigid motions. A network is said to be minimally rigid or isostatic when its total number of degrees of freedom (dN) and constraints (N_e that is the number of edges) are balanced in a way that the number of floppy modes, F, are exactly zero. The Maxwell count for an isostatic *periodic* network (meaning that the network is repeated in all d directions to cover the entire space) is given by:

$$F = dN - N_e - d = 0 \tag{1}$$

with the dimension $d = 2$ in this paper. The last term is to make sure that the d macroscopic translations are properly accounted

a Department of Physics, Arizona State University, Tempe, AZ 85287-1504, USA. E-mail: varda.faghirhagh@asu.edu

b Department of Physics and Materials Science Institute, University of Oregon, Eugene, Oregon 97403, USA.

c Department of Mathematics, University of Tennessee, Knoxville, TN 37996, USA.

d Rudolf Peierls Centre for Theoretical Physics, University of Oxford, 1 Keble Rd, Oxford OX1 3NP, England.

for. All the constraints are assumed to be independent. If a network has any number of edges in excess of isostaticity, it is said to be over-constrained [15].

The network embedding of a jammed system created in periodic boundary conditions has exactly one edge in excess of isostaticity, meaning that there is only one state of self stress in the system. A *self stress* is a state in which the edges are under compression or tension while the net force on each vertex is zero. This extra edge condition is necessary for the mechanical stability and a finite bulk modulus [15,16]. We will refer to this as *isostatic plus one*. We note that this is often referred to confusingly as isostatic in the literature and we strongly discourage this usage. These systems are delicately balanced and a single edge present at isostaic plus one does make a global difference at the isostatic point; no matter how large the system.

In this paper, we define a jammed network as being at *isostatic plus one excess contact* [17,18] and having a *finite bulk modulus*. By finite we mean $O(1)$ and not $O(1/N)$ which will go to zero as the number of vertices N tends to infinity. When one edge is removed from such a network, the network becomes isostatic everywhere, with no stressed edges. We refer to this as *locally isostatic* [19]. This is a stricter requirement than just applying Eq. (1) once globally, as it requires that all subgraphs are also isostatic. Clearly just applying Eq. (1) globally could give rise to subgraphs containing states of self stress that are balanced by other regions containing floppy modes and hinges, as happens when the edges are randomly removed from a highly over-constrained spring network [20].

With this definition, we are now free to adopt any construction method that will achieve this. There is the traditional method which packs particles together by compression and a new method described here. Other definitions of jammed systems are available (see Theorem 1 in ref. [21]) but we have found the above to be the most useful in practice. Note that with the two main properties in this definition, making jammed networks without packing physical particles together is not a trivial process. Because as stated above, building spring networks by adding edges randomly to a distribution of vertices or removing edges randomly from a network that is above isostaticity, does not necessarily result in a network with exactly one state of self stress and a finite bulk modulus of $O(1)$ [20]. It is important to note that for randomly diluted spring networks at the transition point, the ratio of the shear modulus to the bulk modulus is not zero but finite [22]. In order to achieve a zero value for the ratio of the shear to bulk moduli, it is necessary to go beyond random dilution of network models to introduce a global self-organization into the network and methods to do this appropriately are introduced in this paper.

The goal of this paper is to point out the fundamental importance of the two properties used in the new definition. This is achieved by first showing that a special procedure is required to build spring networks that hold these properties and then by showing that networks with these properties display all the other physical properties of jammed networks. Most work on jamming has focused on the compressive packing of objects like disks and spheres, while the jamming phenomenon is much more general. Therefore it is important to be able to prepare jammed systems in different ways that avoid compressive packing. This has some ma-

jor benefits, perhaps of most importance is it broadens our viewpoint as to which materials belong in the class of jammed materials and why they should have similar properties. It also explicitly highlights the role of geometry and global self-organization which is not always so clear in the compressed jammed packs.

2   A New Approach to Jamming

Traditional computational methods available to create jammed packings, usually with disks or spheres, include some mixture of molecular dynamics, event driven dynamics, and energy minimization schemes [18,23–27]. The new method introduced here, produces a jammed network with precisely one state of self stress and expands the set of what was previously accepted as jammed. The new approach uses an algorithm that allows for precise control over the number of contacts in excess of isostaticity [28–30]. We focus on the network as being fundamental to the jammed state and show that in two dimensions, the network can always be replaced by a disk pack, as well as vice-versa.

For a non-crystalline system to be jammed it is necessary but not sufficient for it to be isostatic plus one. An additional degree of cooperativity needs to be introduced by demanding that the bulk modulus drops from finite to zero as a single edge is removed in going from isostatic plus one to the isostatic state. A locally isostatic network can be easily achieved by randomly removing stressed edges from a highly over-constrained network, but the resulting network will not necessarily have a finite bulk modulus at isostatic plus one [20]. Therefore the finiteness of bulk modulus does *not* follow from the system being locally isostatic when an edge is removed. A convenient way to characterize the extreme cooperativity of jammed networks is through two indexes s and h, where s measures the fraction of stressed edges, when any one additional edge is added to an isostatic network, and h measures the fraction of hinged vertices when any one edge is removed. This comes entirely from the static properties, using a standard integer algorithm named pebble game [22,31], and is a very convenient way to establish the marginality of jammed networks without getting into the details of low frequency dynamics [32,33] which is discussed in detail in section 5. If rattlers are removed, both locally isostatic and jammed networks can have $s = 1$ and $h = 1$ [20,34], so this cannot be used to distinguish between them. Hence we need to include in the definition of jammed states that the bulk modulus is finite at isostatic plus one.

The new method to generate polydisperse jammed packs at zero temperature does not require exploring the entire energy landscape to bring the system into zero internal energy and isostaticity. Instead, it builds the system within a single local energy minimum. We try to keep cavities to a minimum so all packing fractions are within the range $0.77 < \phi < 0.82$ after removing the rattlers.

3   Computational Method

This new method is based on a pruning algorithm that is used to manipulate and control the elastic properties of disordered harmonic spring networks [35]. These disordered networks are usually created by minimizing the energy of N repulsive frictionless particles in a periodic box and stopping at a coordination that is

(a)   (b)   (c)
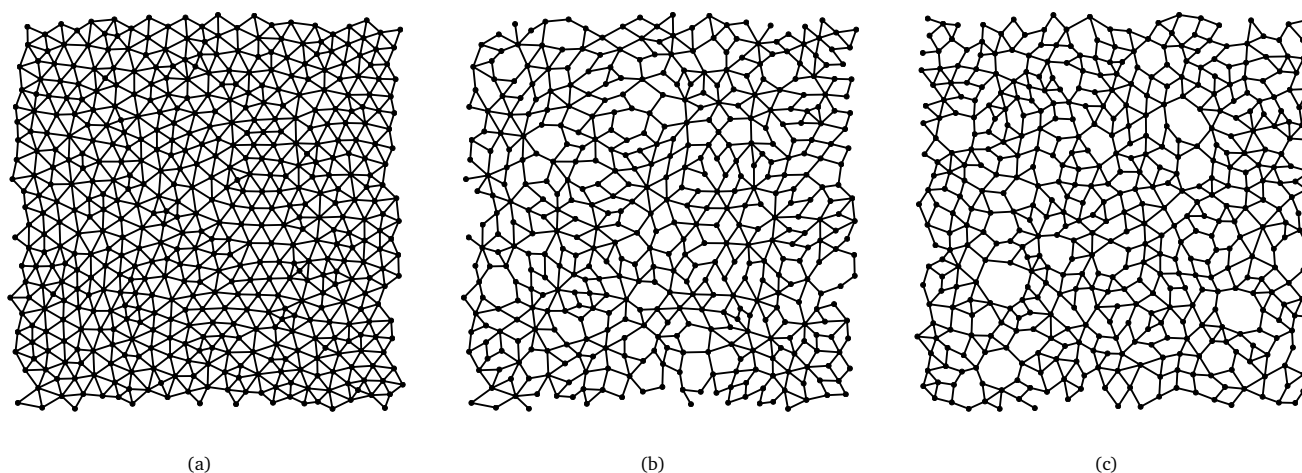
Fig. 1 a) Delaunay triangulation of a Poisson disk sampling with 512 points. b) The same network at the isostatic plus one, after pruning edges that minimally reduce the bulk modulus and removing the rattlers. c) The network representation of a polydisperse jammed pack, formed by compressing disks, with approximately same number of vertices as in part (b).
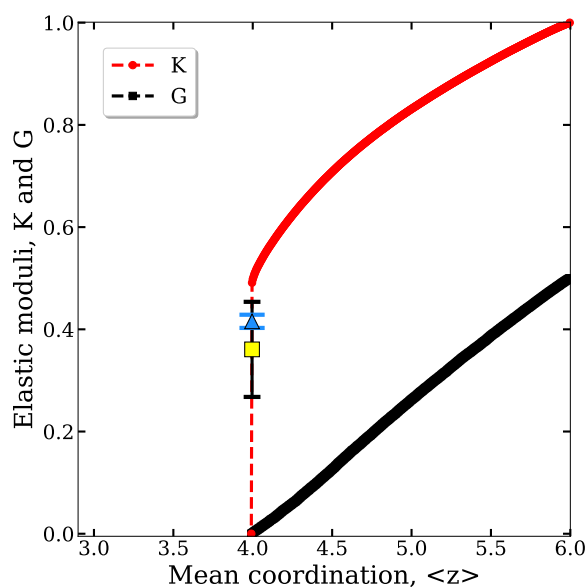

Fig. 2 The ensemble averaged bulk K (red) and shear G (black) elastic moduli of 100 samples with 512 vertices as the edges are removed from mean coordination $\langle z \rangle = 6$ down to $\langle z \rangle \simeq 4$. Both moduli are dimensionless as all the spring constants are made equal and the moduli are normalized so that $K = 1$ at $\langle z \rangle = 6$. The yellow square, with a wide spread, shows the average of bulk moduli for 100 samples generated by `CirclePack`. The blue triangle, with a tighter spread, shows the average of bulk moduli at isostatic plus one for 100 samples generated by conventional jamming algorithms. The jammed systems have the same disk size distribution as circle packings.

summary of the procedure is presented below:

- We start by generating N points in a box with periodic boundary conditions that are distributed by Poisson disk sampling[36,37]. The Poisson sampling is used for aesthetic purposes only and is not necessary for the process. We have confirmed that the same results are obtained when a uniform distribution of points is used.

- We then find the Delaunay triangulation of these points[38]. To make the triangles look more regular, we move each vertex to the centroid of the polygon formed by its nearest neighbors, iteratively, until every vertex is at the centroid of its neighbors. This step, is again for aesthetic purposes and does not affect the final results reported in this paper. An example of such generated samples is shown in Figure 1-a. This geometrically generated network is highly over-constrained and far from isostatic (with a mean coordination of $\langle z \rangle = 2N_e/N = 6$), therefore we need to remove N_r redundant edges to push it down to the isostatic plus one point as desired.

- There are $\binom{N_e}{N_r}$ ways to prune these N_r redundant edges from the network. It is well known[39,40] that the contribution of a removed edge to the bulk modulus is largely independent of its contribution to the shear modulus, although these moduli cannot increase by removing an edge ([41], pp. 110-111). Since jammed packs maintain a finite bulk modulus while the ratio of shear (G) and bulk (K) moduli vanishes at jamming point, at each step we find and remove the edge that maximizes the bulk modulus of the remaining network. Maximizing the bulk modulus is not strictly necessary as similar results can be obtained if we remove an edge randomly from the top 20% of edges that have minimal contribution to the changes in bulk modulus.

- We repeat the process, until we arrive at isostatic plus one

slightly above jamming transition point. Therefore they already have encoded in them the properties of jamming and should not be thought of as generic networks. By contrast, in this work we generate the initial networks *de novo and far from jamming*, using computational geometry only. The disordered jamming-like networks are then created by performing a simple set of steps. A

where $\langle z \rangle \simeq 4$. The resulting network has a finite bulk modulus and is shown in Figure 1-b. Figure 2 shows how the bulk and shear elastic moduli of the network change as the edges are pruned. The behavior of the shear modulus is reminiscent of random rigidity percolation models[20] as well as jamming.

4 Results

At this point we have a spring network that is identical to the network representation of a jammed pack (an example is shown in Figure 1-c) in all the following aspects (none of which holds for a percolating rigid network at the marginal point):

1. The network has one excess contact past mathematical isostaticity (isostatic plus one),

2. The bulk modulus of the network is finite and $O(1)$,

3. The ratio of shear and bulk elastic moduli (G/K) scales as $\Delta z = \langle z \rangle - z_J$ where z_J is the mean coordination at the marginal point,

4. It is marginal, as both its s and h indexes are equal to 1[34] and there is an excess of low excitation vibrational modes in their density of states similar to that of a jammed system as is shown in section 5

5. It is stable as revealed by the study of its dynamical matrix. All of the eigenvalues are positive (except for the two trivial translational eigenvectors whose eigenvalues are zero).

6. 100% of the forces due to the single state of self stress in the network are positive definite and their distribution looks similar to the force distribution of jammed systems (see section 6). This is very different from randomly pruned networks at the critical point where the fraction of compressive forces is about 50%.

The next step realizes this periodic network as a circle packing on a geometric torus (alternately called a disk pack[42]). Our approach, in essence, replaces the interactions between particles, which are represented by springs, by the interactions between circles, which are based on well understood geometric principles. The methods come from a topic called circle packing, which was introduced by William Thurston[43,44]; the standard reference is [45], see in particular Chapter 9, and the computations are carried out in the software `CirclePack`[46].

A "circle packing" is a configuration of circles (or disks) which realizes a prescribed pattern of tangencies. In our models, information about circles that are tangent to one another is encoded in the given periodic network, which is treated as a graph on a topological torus. Each particle, a vertex in the network, will be represented by a circle, and if two particles are connected by an edge in the network, then their circles are required to be tangent in the associated circle packing. Computations, however, require a graph which is a triangulation. Generically, our networks will not be triangulations since we have to prune one third of the edges from an original triangulation to get to the isostatic
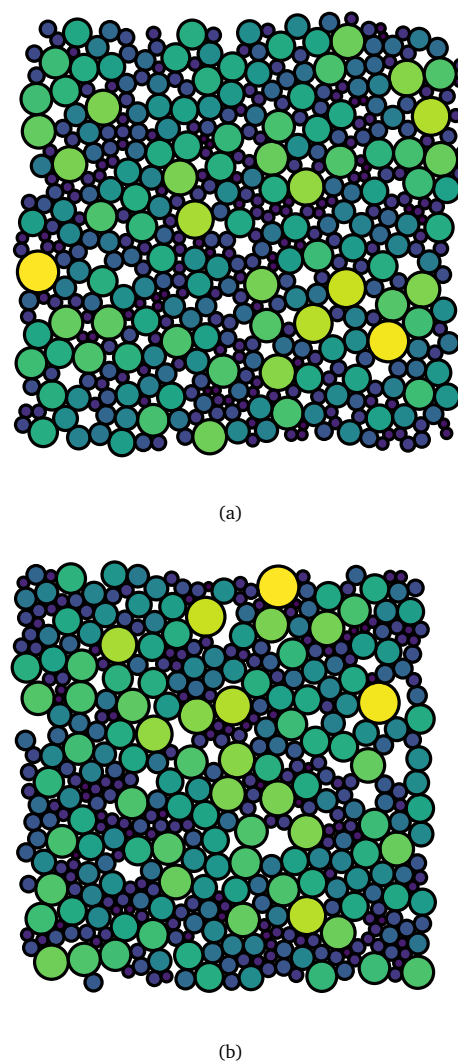

(a)

(b)

Fig. 3 a) Packing generated by the pruning algorithm and `CirclePack` b) Rattler free packing generated by standard algorithms.

plus one point. So, in any face bounded by four or more edges, we temporarily introduce a single auxiliary vertex connected to each of the network vertices defining that face. This augmented network is a triangulation of a topological torus, and circle packing theory (see[47] and[45][Prop 9.1]) guarantees the existence of a geometric torus and an associated circle packing on that torus. This is where `CirclePack` comes in: it first computes the radii of all the circles, then using these and the pattern of tangencies of the triangulation, it lays the circles out as a periodic circle packing in the plane. The periodicity determines the geometric torus on which the packing lives. Discarding the disks for the auxiliary vertices leaves a circle packing with locations and radii for the vertices of the original network, as in Figure 3-a.

There are two things to note about our computations. First, theory guarantees that each computed circle packing is unique up to scaling and rigid motions, that is, up to uniform scaling of all radii and rotating or translating the configuration. However, uniqueness depends on the method we have chosen for augment-

ing the original network – namely, adding a single vertex in each non-triangular cell. Other options to get triangulations will result in alternative circle packings that satisfy the constraints of the original network. With continued refinement of our methods, one might find physically meaningful options for augmentation or one might add parameters available in more advanced circle packing theory (see[45] [Appendix E]). Second, we point out that there are infinitely many distinct geometric tori. Mathematically these are distinguished by what is known as conformal structure (see, e.g.[48]); in practice, they are distinguished by the periodicity of their layout in the plane. `CirclePack` computations yield a unique geometric torus for each of our circle packings (depending on triangulation as noted above). In the absence of anisotropy, i.e., with materials having no preferred directions, the geometries of the computed torus do not appear to us to be physically pertinent.

`CirclePack` changes the geometrical configuration of vertices. However, the connectivity of the system does not change and the bulk modulus remains finite after this transformation with a standard deviation of $s = 0.09$ for the samples studied here, as can be seen in Figure 2.

The generated circle packing holds all but one of the properties of the pruned networks discussed above. It is at isostatic plus one, has a finite bulk modulus of $O(1)$ and a vanishingly small shear modulus of $O(1/N)$. It is also marginal with $s = h = 1$, and stable which means it would not change for a small enough compress-decompress protocol. The difference is that not all the forces due to the single state of self stress in the system (although a majority of 72% to 99% of them in the samples studied here) are necessarily positive definite (item 6 above). This comes as a result of our non-unique mapping from the network to the disk packing. A visualization of this type of change in the state of self stress of a network can be found in section 6.

Every circle packing has a distribution of radii that can be assigned to particles in a standard molecular dynamics simulation to generate a polydisperse 2D disk packing that can be compared to the packing generated by the newly introduced algorithm. In this approach, we first scale the radii of particles to achieve a starting packing fraction well above the jamming transition; typically packing fraction $\phi_J \simeq 0.85$ for disks. Particles interact through a standard contact harmonic potential. The system is minimized to its inherent structure at this initial density using a quad-precision GPU implementation of the FIRE algorithm[30,49]. Configurations at a desired excess number of contacts can be achieved by exploiting the scaling of total energy $U \propto (\phi - \phi_J)^2$, where ϕ_J is the isostatic jamming density. The system is successively brought to lower energies and thus lower numbers of excess contacts by rescaling the radii and re-minimizing. The rescalings are chosen to achieve approximately 10 steps per decade of $\phi - \phi_J$. This process continues until the number of excess contacts is reduced to the desired value. At each density the number of excess contacts is calculated on the rigid core of the system by first removing *rattler* particles lacking at least $d + 1$ non-cohemispheric contacts. The blue triangle in Figure 2 shows the average bulk modulus of 100 samples generated by this method. The standard deviation is in order of $s = 0.01$, which is smaller than the stan-
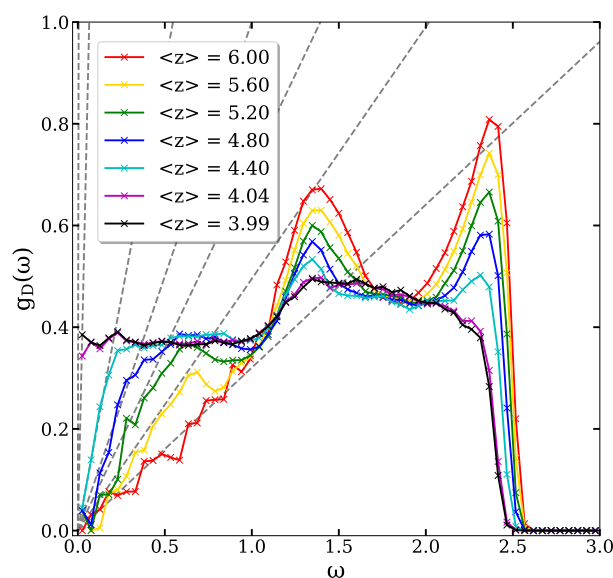
dard deviation obtained from results of `CirclePack`.

Fig. 4 (color online) The evolution of probability density function for acoustic modes in disordered spring networks as the bonds are pruned from $\langle z \rangle = 6$ down to $\langle z \rangle \approx 4$ (isostatic plus one) while keeping the bulk modulus finite. The dashed lines display Eq. (6) for the average elastic moduli associated with each value of $\langle z \rangle$ shown on the colored curves. The results are ensemble averaged over 100 samples, each with 512 vertices.

There are measurables that are not universal - like the density, pair distribution function, etc. These vary widely for conventional jammed packs as well as in the jammed systems here, depending largely upon the number of rattlers, the size of convex cavities that are present, and the protocol that is being used to generate the jammed packs. For instance, the average packing fraction of 100 test samples generated by `CirclePack` is $\phi \simeq 0.77$ which is lower than that of samples generated by our standard algorithm where $\phi \simeq 0.82$ after removing the rattlers. We emphasize again that the circle packing construction used here is not unique and does not create packings with all positive definite forces. This then explains the lower density as it is well known that attractive interactions (or indeed frictional interactions) allow one to create critically jammed packings at significantly lower densities[50]. The precise ways the disks of various radii are located is also not a crucial issue and can vary from well mixed to some clustering. Figure 3 shows the comparison of two samples with 512 particles.
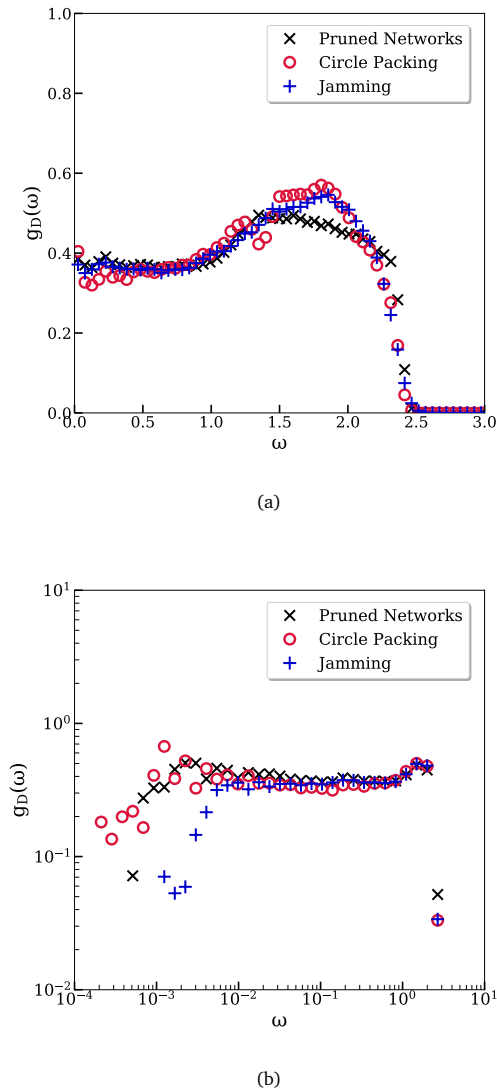
(a)

(b)

Fig. 5 (color online) a) The probability density function for vibrational modes in 2D pruned networks (blue), their equivalent circle packs (red) and jammed systems (black) in linear scale. b) The plot of part (a) in logarithmic scale.

5 Comparison of the Vibrational Modes

One of the most important features of disordered systems such as glasses and jamming is the excess of low frequency phonon modes in their density of vibrational states compared to Debye's prediction for crystalline solids (Boson peak)[7–9]. Here we look into the density of states (DOS) in the pruned network constructions and their equivalent circle packs and compare the results to physically jammed systems. First, we study the evolution of DOS in the disordered networks as they are pruned from $\langle z \rangle = 6$ to $\langle z \rangle \approx 4$. For a 2D spring network of area A, the number of allowed wave modes between wave numbers 0 and q is[51]:

$$n(q) = \frac{A}{(2\pi)^2}\pi q^2 \qquad (2)$$

We assume the vibrational frequencies are low enough for the

dispersion relation to be almost linear for both longitudinal (L) and transverse (T) acoustic modes:

$$q = \frac{\omega}{v_\alpha} \qquad (3)$$

where $\alpha = T, L$. This means the number of vibrational modes $n(\omega)$ is quadratic in frequency which leads to the following form for density of states:

$$\mathscr{D}(\omega) = \frac{dn(\omega)}{d\omega} = \frac{A}{2\pi v_\alpha^2}\omega \qquad (4)$$

On the other hand, the longitudinal and transverse sound velocities are related to the bulk (K) and shear (G) moduli of a 2D spring network in the following form:

$$v_L = \sqrt{\frac{G + K}{\rho}}$$

$$v_T = \sqrt{\frac{G}{\rho}} \qquad (5)$$

where $\rho = N/A$ is the mass density. Here the mass density is equal to the number density of the system since all vertices have unit mass. By inserting Eq. (5) into Eq. (4) and using the normalization $g_{\mathscr{D}}(\omega) = \mathscr{D}(\omega)/N$ so that $\int g_{\mathscr{D}}(\omega)\,d\omega = 1$, we can write the probability distribution function of the vibrational modes in terms of the elastic moduli of the system[52]:

$$g_{\mathscr{D}}(\omega) = \frac{\omega}{2\pi}\left(\frac{1}{G} + \frac{1}{G + K}\right) \qquad (6)$$

The linearity of $g_{\mathscr{D}}(\omega)$ versus ω is the Debye-like low frequency behavior that is expected to be seen in any material with non-zero values of sound velocities. This is observed for networks far from marginality in the lower left corner of Figure 4. When the edges with smallest contribution to the bulk modulus are removed from a fully triangulated disordered spring network, the shear modulus approaches zero almost linearly, while the bulk modulus remains finite. Therefore the first term on the RHS of Eq. (6) diverges and the density of states becomes flat near the transition point which is a characteristic of the vibrational modes in disordered systems at their marginal transition point[1,52,53].

Figure 5 shows the plots of $g_{\mathscr{D}}(\omega)$ for three types of systems studied here: the pruned networks at isostatic plus one, their equivalent circle packings, and the jammed systems generated by using the size distribution of circle packs both in linear and logarithmic scale. The marginality of all these systems is evident by their flat density of states at low frequencies.

6 Comparison of the Force Networks

In this section, we first display a visualization of the changes in the state of self stress of a network before and after running `CirclePack`. Then, we show the distributions of the forces in our studied systems. The transformation of the state of self stress in a network is shown in Figure 6, where the edges that carry a positive definite force are colored in black and edges that carry a negative force are shown in red (the width of each edge is proportional to the magnitude of the force along that edge). As can

be seen from this figure, all the forces in a pruned network are positive definite. Therefore, there are no red edges in the image of panel 6-a. It is only after running the `CirclePack` that tensile forces appear. In Figure 6-b, only 6% of the forces are negative. Note that these two networks have the exact same connectivity and the reason they appear different is because the `CirclePack` algorithm changes the positions of the vertices.
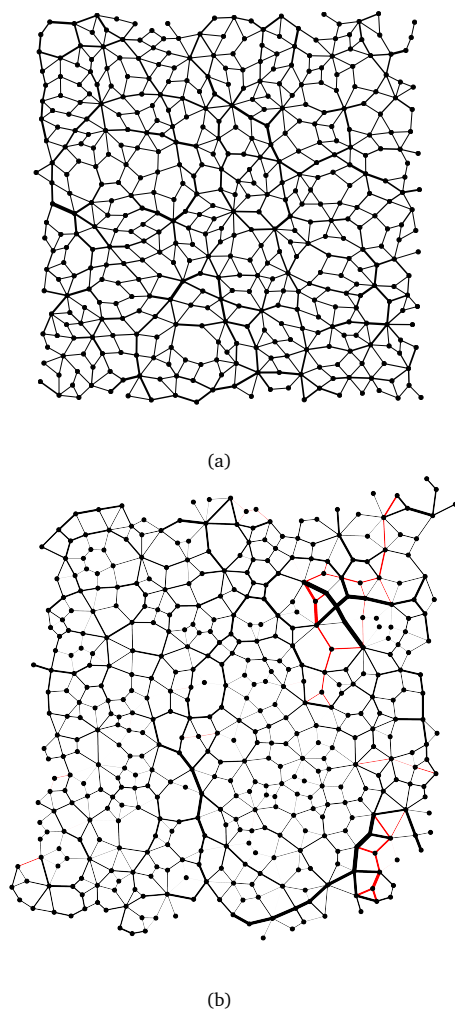
with the mean field full-replica symmetry breaking results[30], as is expected for a jamming transition that happens deep within the marginal glass phase. However, the pruned network has an exponent in the CDF consistent with 1, which matches well with the single-replica symmetry breaking result for stable glasses[54].
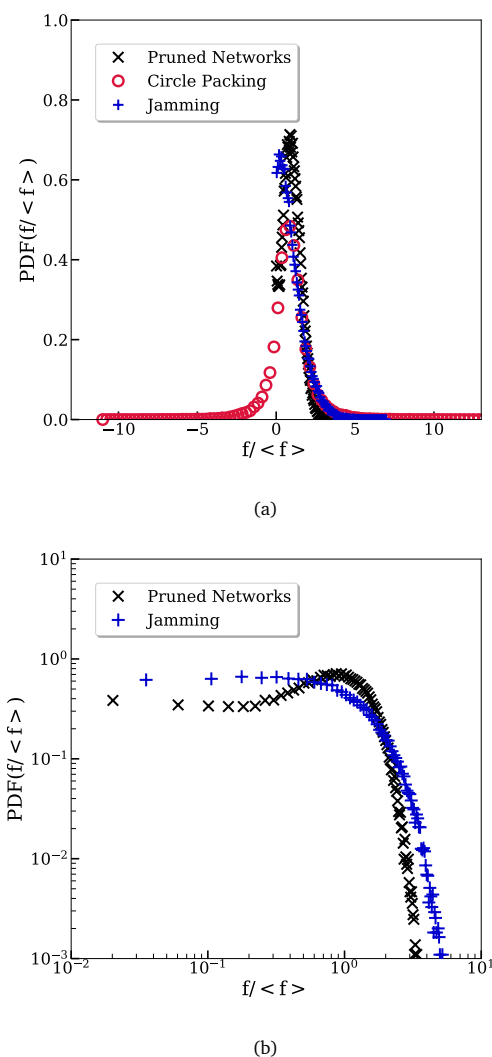

(a)

(b)

Fig. 6 (color online) a) A network created by the pruning algorithm before running the `CirclePack`. The edges with positive definite forces are colored black. There are no edges with negative forces in this network. b) The same network after running the `CirclePack`, which leads to changes in the positions of the vertices. The black edges represent contacts with positive definite forces and the red edges show contacts that carry negative forces. The widths of the lines are proportional to the magnitudes of the forces.

Figure 7 shows the probability distribution of forces in the single state of self stress at isostatic plus one for the pruned networks, circle packings, and jammed systems. The logarithmic plot in panel 7-b shows this probability distribution for pruned networks and jamming only. While they look quite similar on this scale, a plot of the cumulative distribution of forces (Figure 8) reveals an intriguing distinction. The physically jammed packing has a low force scaling exponent for all forces that is consistent

(a)

(b)

Fig. 7 (color online) a) The probability distribution function of forces for pruned networks, circle packings, and jammed systems at isostatic plus one. b) The force probability distribution functions in a logarithmic scale for pruned networks and jammed systems only. Both exhibit a nearly constant distribution of forces for small forces.
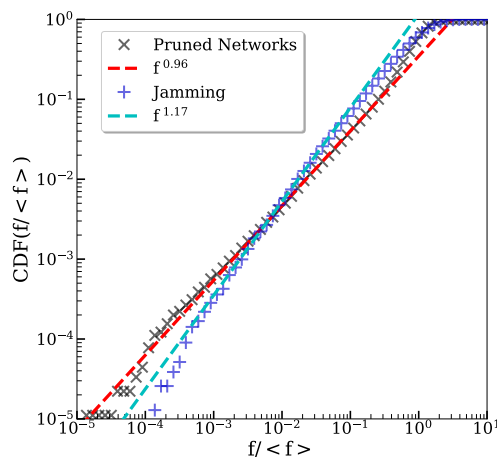
Fig. 8 (color online) The cumulative distribution function of forces for pruned networks and jamming at isostatic plus one. Best fit power laws are over plotted in red for the pruned networks and teal for the jammed systems.

7   Discussion

In this paper, we have shown that the essence of the jamming transition is the underlying network involved at the isostatic plus one point. But another ingredient is required - that the bulk modulus goes from a finite value to zero as one constraint is removed to take the network from isostatic plus one to isostatic. This not only clarifies the nature of the jamming transition, but shows that conventionally jammed networks (formed by compacting particles together) are part of a larger group of networks controlled by topology with the added cooperative geometric ingredient that the bulk modulus remains finite. Such cooperativity is essential to make the network jammed, and much more restrictive than merely being isostatic. We have also demonstrated that all of the interesting macroscopic properties of jammed matter derive from the marginality of the system and its bulk mechanical properties. As such, both our generated networks and their equivalent circle packings behave as properly jammed systems for all bulk interrogations. However, the microscopic properties of jamming are only satisfied by the pruned networks and not the circle packs. This is because the force distributions in pruned networks and jamming follow similar scaling laws, whereas the circle packings fail to do so since forces are not positive everywhere. We note finally that in all the networks discussed in this paper, the shear modulus goes from $O(1/N)$ at isostatic plus one, to zero at isostatic. The ideas in this paper generalize easily to any dimensions, but the final step of going from a network to a hypersphere pack is only possible in 2D.

8   Conflicts of interest

There are no conflicts to declare.

9   Acknowledgements

References

1   M. Van Hecke, *Journal of Physics: Condensed Matter*, 2009, **22**, 033101.

2   F. Bolton and D. Weaire, *Physical review letters*, 1990, **65**, 3449.

3   J. G. Puckett, F. Lechenault and K. E. Daniels, *Physical Review E*, 2011, **83**, 041301.

4   C. Brito and M. Wyart, *EPL (Europhysics Letters)*, 2006, **76**, 149.

5   A. J. Liu and S. R. Nagel, *Nature*, 1998, **396**, 21.

6   C. S. OâĂŹhern, L. E. Silbert, A. J. Liu and S. R. Nagel, *Physical Review E*, 2003, **68**, 011306.

7   T. Grigera, V. Martin-Mayor, G. Parisi and P. Verrocchio, *Nature*, 2003, **422**, 289.

8   N. Xu, M. Wyart, A. J. Liu and S. R. Nagel, *Physical review letters*, 2007, **98**, 175502.

9   N. Xu, V. Vitelli, M. Wyart, A. J. Liu and S. R. Nagel, *Physical review letters*, 2009, **102**, 038001.

10   S. Alexander, *Physics reports*, 1998, **296**, 65–236.

11   M. Wyart, *arXiv preprint cond-mat/0512155*, 2005.

12   H. He and M. F. Thorpe, *Physical Review Letters*, 1985, **54**, 2107.

13   W. G. Ellenbroek, Z. Zeravcic, W. van Saarloos and M. van Hecke, *EPL (Europhysics Letters)*, 2009, **87**, 34004.

14   V. F. Hagh, *Ph.D. dissertation*, Arizona State University, 2018.

15   M. F. Thorpe, *Encyclopedia of Complexity and Systems Science*, Springer, 2009, pp. 6013–6024.

16   E. Guyon, S. Roux, A. Hansen, D. Bideau, J.-P. Troadec and H. Crapo, *Reports on Progress in Physics*, 1990, **53**, 373.

17   S. Dagois-Bohy, B. P. Tighe, J. Simon, S. Henkes and M. Van Hecke, *Physical review letters*, 2012, **109**, 095703.

18   C. P. Goodrich, A. J. Liu and S. R. Nagel, *Physical Review Letters*, 2012, **109**, 095704.

19   L. Theran, A. Nixon, E. Ross, M. Sadjadi, B. Servatius and M. F. Thorpe, *Physical Review E*, 2015, **92**, 053306.

20   W. G. Ellenbroek, V. F. Hagh, A. Kumar, M. Thorpe and M. Van Hecke, *Physical review letters*, 2015, **114**, 135501.

21   R. Connelly, E. Solomonides and M. Yampolskaya, *arXiv preprint arXiv:1702.08442*, 2017.

22   D. J. Jacobs and M. F. Thorpe, *Physical review letters*, 1995, **75**, 4051.

23 C. S. O'Hern, S. A. Langer, A. J. Liu and S. R. Nagel, *Physical Review Letters*, 2002, **88**, 075507.

24 A. Donev, S. Torquato and F. H. Stillinger, *Physical Review E*, 2005, **71**, 011105.

25 A. J. Liu and S. R. Nagel, *Annu. Rev. Condens. Matter Phys.*, 2010, **1**, 347–369.

26 S. Torquato and Y. Jiao, *Physical Review E*, 2010, **82**, 061302.

27 E. Lerner, G. DÃijring and M. Wyart, *Soft Matter*, 2013, **9**, 8252–8263.

28 P. Charbonneau, E. I. Corwin, G. Parisi and F. Zamponi, *Physical Review Letters*, 2012, **109**, 205501.

29 P. K. Morse and E. I. Corwin, *Physical Review Letters*, 2014, **112**, 115701.

30 P. Charbonneau, E. I. Corwin, G. Parisi and F. Zamponi, *Physical Review Letters*, 2015, **114**, 125504.

31 D. J. Jacobs and B. Hendrickson, *Journal of Computational Physics*, 1997, **137**, 346–365.

32 M. Wyart, S. R. Nagel and T. A. Witten, *EPL (Europhysics Letters)*, 2005, **72**, 486.

33 L. E. Silbert, A. J. Liu and S. R. Nagel, *Physical review letters*, 2005, **95**, 098301.

34 When pruning a spring network, if we do not remove the rattlers that appear in the form of vertexes with coordination number $z = 2$, the s and h indexes will be slightly smaller than 1.

35 C. P. Goodrich, A. J. Liu and S. R. Nagel, *Physical review letters*, 2015, **114**, 225501.

36 R. Bridson, SIGGRAPH sketches, 2007, p. 22.

37 D. Dunbar and G. Humphreys, ACM Transactions on Graphics (TOG), 2006, pp. 503–508.

38 D.-T. Lee and B. J. Schachter, *International Journal of Computer & Information Sciences*, 1980, **9**, 219–242.

39 D. Hexner, A. J. Liu and S. R. Nagel, *Soft matter*, 2018.

40 D. Hexner, A. J. Liu and S. R. Nagel, *arXiv preprint arXiv:1706.06153*, 2017.

41 J. Lord Rayleigh, *The theory of sound, vol. 1*, 1945.

42 J. H. Lopez, L. Cao and J. Schwarz, *Physical Review E*, 2013, **88**, 062130.

43 W. Thurston, *The Geometry and Topology of 3-Manifolds*, Princeton University Notes.

44 W. Thurston, *The finite Riemann mapping theorem*, 1985, Invited talk, An International Symposium at Purdue University in celebrations of de Branges' proof of the Bieberbach conjecture, March 1985.

45 K. Stephenson, *Introduction to Circle Packing: the Theory of Discrete Analytic Functions*, Camb. Univ. Press, New York, 2005.

46 K. Stephenson, `CirclePack` *Software*, 1992–, http://www.circlepack.com/software.html.

47 A. F. Beardon and K. Stephenson, *Indiana Univ. Math. J.*, 1990, **39**, 1383–1425.

48 G. A. Jones and D. Singerman, *Complex functions: an algebraic and geometric viewpoint*, Cambridge university press, 1987.

49 E. Bitzek, P. Koskinen, F. GÃd'hler, M. Moseler and P. Gumbsch, *Physical Review Letters*, 2006, **97**, 170201.

50 D. J. Koeze and B. P. Tighe, *Physical review letters*, 2018, **121**, 188002.

51 C. Kittel, P. McEuen and P. McEuen, *Introduction to solid state physics*, Wiley New York, 1996, vol. 8.

52 L. Zhang, J. Zheng, Y. Wang, L. Zhang, Z. Jin, L. Hong, Y. Wang and J. Zhang, *Nature communications*, 2017, **8**, 67.

53 P. Charbonneau, E. I. Corwin, G. Parisi, A. Poncet and F. Zamponi, *Physical review letters*, 2016, **117**, 045503.

54 S. Franz and G. Parisi, *Journal of Physics A: Mathematical and Theoretical*, 2016, **49**, 145001.